

Microvasculature of the Buffalo (*Bubalus bubalis*) Choroid Plexuses: Structural, Histochemical, and Immunocytochemical Study

GAETANO SCALA,^{1*} MARIO CORONA,² EMILIA LANGELLA,³ AND LUCIANNA MARUCCIO¹

¹Department of Biological Structures, Functions and Technologies, University of Naples Federico II, Italy

²Department of Soil, Plant, Environment and Animal Production Sciences, University of Naples Federico II, Italy

³Department of Animal Production Sciences, University of the Basilicata, Potenza, Italy

KEY WORDS buffalo; choroid plexuses; SEM vascular corrosion casts; TEM; NADPHd; immunogold NOS I

ABSTRACT The choroid plexuses (CPs) in mammals produce the cerebrospinal fluid (CSF). In the literature, the morphology of CPs and the process that regulates the production of CSF are virtually nonexistent for domestic ruminants. Thus this study has two aims: 1. to investigate the morpho-structure of the buffalo CP microvasculature utilizing light microscopy (LM), scanning electron microscopy (SEM) and transmission electron microscopy (TEM) techniques, and 2. to investigate the relationship between the blood vessels and both the elongated cells and the cells with multiple protrusions located in the CPs. SEM and TEM analyses of the CPs from buffalo brain showed morphological and structural features similar those reported in other mammalian species. Moreover the blood microvasculature is the major component responsible for the formation of the CSF, secreted by the encephalic CPs. In addition the chemical composition of this fluid depends on several morpho-functional characteristics of the vascularization of the CPs. These characteristics are as follows: two shapes of the vascular organization: lamina-like and ovoid-like elongated cells of the CPs, which connect the ventricular cavities to the blood capillaries; and the CP capillaries have diverse forms. In the present study the employment of NADPHd and NOS I was taken as indirect evidence for the presence of NO for investigation their specific role in CPs. Then NOS I immunoreactivity is found in the walls of CP blood vessels demonstrating indirectly the presence of NO with a vaso-dilatatory and autoregulation function of vascular tone by cholinergic nerve stimulation of blood vessel smooth muscle. *Microsc. Res. Tech.* 74:67–75, 2011. © 2010 Wiley-Liss, Inc.

INTRODUCTION

The choroid plexuses (CPs) in mammals are aggregations of blood vessels covered with choroid epithelium, which control the homeostasis of the central nervous system (CNS). They also produce about 90% of the cerebrospinal fluid (CSF) through secretion and absorption processes. The CSF is in direct contact with the interstitial fluid of nerve structures, and is indispensable to the maintenance of cerebral function. This implies that damage to the CNS structures may cause pathologies, and underscores the importance of precise and detailed knowledge of the CPs for eventual clinical applications. The morphology, structure and function of mammalian CPs have been studied, but data regarding the CPs cellular elements, and the process that regulates the production of CSF are virtually nonexistent for domestic ruminants. The information in the literature consists of (1) a SEM study of sheep CPs (Rajtová, 2002); (2) a microvascular description of the lateral ventricles in goat (Scala et al., 1994); (3) a scanning and transmission microscopy study of two heretofore unknown cellular types, i.e., elongated cells and cells with multiple protrusions, from the CPs of buffalo (Scala et al., 2007); and (4) two immuno-histochemical studies in the CPs of buffalo (Pavone et al., 2007; Tafuri et al., 2009). As of yet there have been no mor-

pho-structural studies of the blood vessels that comprise the CPs. The present study has two aims: (1) to investigate the morpho-structure of the buffalo CP microvasculature utilizing light microscopy (LM), scanning electron microscopy (SEM) and transmission electron microscopy (TEM) techniques, and (2) to investigate the relationships between the blood vessels and both the elongated cells and the cells with multiple protrusions located within the CPs.

This study employed NADPH diaphorase (NADPHd) and neuronal nitric oxide synthase (NOS) as indirect evidence for NO in order to investigate their specific role in CPs. Several studies have provided direct evidence for a specific role of nitric oxide (NO) in the CNS of mammals (Feldman et al., 1993; Dawson and Dawson, 1996). The cytoplasm cellular of choroid plexus present cGMP and cGMP-dependent protein kinase (Cumming et al., 1981) and the activation of cGMP-dependent protein kinase has been shown to regulate Ca²⁺ homeostasis which influences vascular tone

*Correspondence to: Prof. Gaetano Scala, University of Naples Federico II, Department of Biological Structures, Functions and Technologies, Via Veterinaria, 1-80137 Naples, Italy. E-mail: gaescala@unina.it

Received 1 March 2010; accepted in revised form 6 April 2010

DOI 10.1002/jemt.20875

Published online 13 May 2010 in Wiley Online Library (wileyonlinelibrary.com).

(Moncada and Higgs, 2006). Furthermore, cGMP-dependent activation of membrane channels regulates CSF homeostasis (Hirooka et al., 2000). NADPHd activity was also found in the neurons along with NOS. The form of NADPHd in neurons is identical to NOSI (Hope et al., 1991).

MATERIALS AND METHODS

Animals

Thirty-three heads were collected immediately after slaughter from adult buffaloes (*Bubalus bubalis*). From animal brains CPs were collected and processed in a different way depending on the type of microscopy to be used.

SEM-Vascular Corrosion Cast and Intact Tissue Technique

SEM analysis was performed on CP samples obtained by two distinct procedures: 1. vascular corrosion cast technique, and 2. intact tissue technique. 1. In the case of vascular corrosion cast technique, six heads were perfused through the maxillary artery with a 0.9% physiological saline for cleaning of the vascular system. They were then injected with a low-viscosity, colored methacrylate mixture to obtain a cast of CPs (Ohtani et al., 1982). The brains were soaked in 30% KOH solution for 1–2 weeks, changing the solution every 4–5 days. Upon complete corrosion, the casts were rinsed with bidistilled water, and dried in desiccators. CP casts from lateral, III, and IV ventricles were separated, mounted on stubs (25 mm, diameter), and coated with gold using a sputter coater (SC500, Bio-Rad, Hemel Hempstead, U.K.). All gold-coated samples were examined, and photographed under a scanning electron microscope (LEO 435 VP, Leica, Cambridge, U.K.) at 10 kV. 2. In the case of tissue technique, six heads were perfused through the maxillary artery with 0.1 M phosphate buffered saline (PBS), pH 7.3, and then fixed with Karnovsky's solution (4% paraformaldehyde, 2.5% glutaraldehyde). After 12 h, the brains were removed, and the collected CPs was cut into small fragments (0.5 cm, length). All fragments were immersed in a solution of 4.5% glucose in phosphate buffer, pH 7.3, for 24–48 h, dehydrated in ethyl alcohol, and dried to the critical point (CPD 030, Balzers, Liechtenstein). The specimens were mounted on stubs (12.5 mm, diameter), coated by gold and examined under a LEO 435 VP microscope at 20 kV, and photographed.

Transmission Electron Microscopy

Six heads were perfused through the maxillary artery with 0.1 M cacodylate buffer, pH 7.2, and then fixed with a mixture of this buffer and 2% glutaraldehyde. After 1 h, brains were removed, and the CPs collected. CPs were cut into minute fragments, immersed in glutaraldehyde for 1 h, rinsed in cacodylate buffer, postfixed with 2% OsO₄ for 2 h, dehydrated, and embedded in Embed 812 resin (Electron Microscopy Supplies, Ft. Washington, Pennsylvania 19034). All embedded specimens were sliced into thin sections using an ultramicrotome (Ultratome IV-LKB, Bromma, Sweden), stained with uranyl acetate and lead citrate (Ultrastain-LKB), examined under a transmission electron microscope (Philips EM 201, Eindhoven, The Netherlands) at 40 kV, and photographed.

LM Histochemistry

CPs were immediately removed from the brain of six buffaloes, and cut in small pieces. Samples were washed in 0.1 M PBS, transferred into a graded series of saccharose (10, 20, and 30%), immersed in Tissue teck OCT compound (Sigma Chem., St. Louis, MO), frozen in liquid nitrogen, and sectioned by a cryostat. To evaluate NADPHd activity, sections were incubated with 0.25 mg/mL nitro blue tetrazolium, 1 mg/mL NADPH, and 0.5% Triton X-100 in 0.1 M Tris-HCl buffer, pH 7.3, at 37°C for 10–15 min in a dark box or at room temperature for 30 min. The reaction was stopped by sample immersion in 0.1 M Tris-HCl buffer. Finally, sections were mounted on cover slips, examined under a light microscope (Orthoplan, Leitz GmbH, Wetzlar, Germany), and photographed. Control sections included incubation in media in which substrate was omitted, and preincubation with the sulfhydryl inhibitor, 5.5'-dithio-bis-2-nitrobenzoic acid. None of these controls produced positive staining.

Immunogold-Labeling SEM Analysis

For the immunogold-labeling SEM analysis, CPs were immediately removed from the brain of six animals, and immersed in PBS for 1 h. Samples were incubated for 2 h in a solution containing normal goat serum (X 0907, Dako Italia s.p.a., Milano, Italy) diluted 1:10 in PBS, and then in a primary rabbit polyclonal antibody raised against a peptide mapping the 724–739 amino acid sequence of human brain NOS I (AB1632, Chemicon International, Temecula CA), diluted 1:1,500 in PBS, overnight at 4°C. After washing in PBS, samples were incubated with gold-conjugated goat antirabbit IgG (E.M.GAR10, Agar Scientific Limited, Stansted, U.K.) diluted 1:200 in PBS, for 1 h at room temperature. The secondary antibody was conjugated with gold particles of different size, namely 5 and 15 nm. After washings in PBS, samples were fixed by 2.5% glutaraldehyde in 0.1 M cacodylate buffer containing CaCl₂, pH 7.2, for 30 min. After the fixation step and washings with distilled water, samples were subjected to silver enhancement (British BioCell International, Cardiff, Wales, U.K.). The enhancement process enables the use of antibodies conjugated to smaller (1–5 nm) gold particles, preserving the advantage of faster penetration and higher labeling efficiency (Owen et al., 2002). Next, samples were dehydrated through an ethanol series, and dried to the critical point. The specimens, mounted on stubs, were examined under a LEO 435 VP scanning electron microscope at variable pressure (80–120 Pa) in the backscattered electron mode, which allows detecting gold particles associated to cells even if they are intracellular located (Richards et al., 2001). Samples had not been coated by gold, so that SEM observed the only conjugated gold deriving from immunocytochemical reaction, and photographed.

Western Blotting

CPs removed from three buffalo brains were homogenized by an Ultraturrax L-407 at 4°C with 5 mL/1.5 g tissue of buffer containing 50 mM Tris-HCl, pH 7.4 150 mM NaCl, 1 mM ethylenediaminetetraacetic acid, 10 mM NaF, 0.5% deoxycholic acid, 0.1% sodium dodecyl sulfate (SDS), 1% Nonidet P-40, 1 mM phenylmethyl-

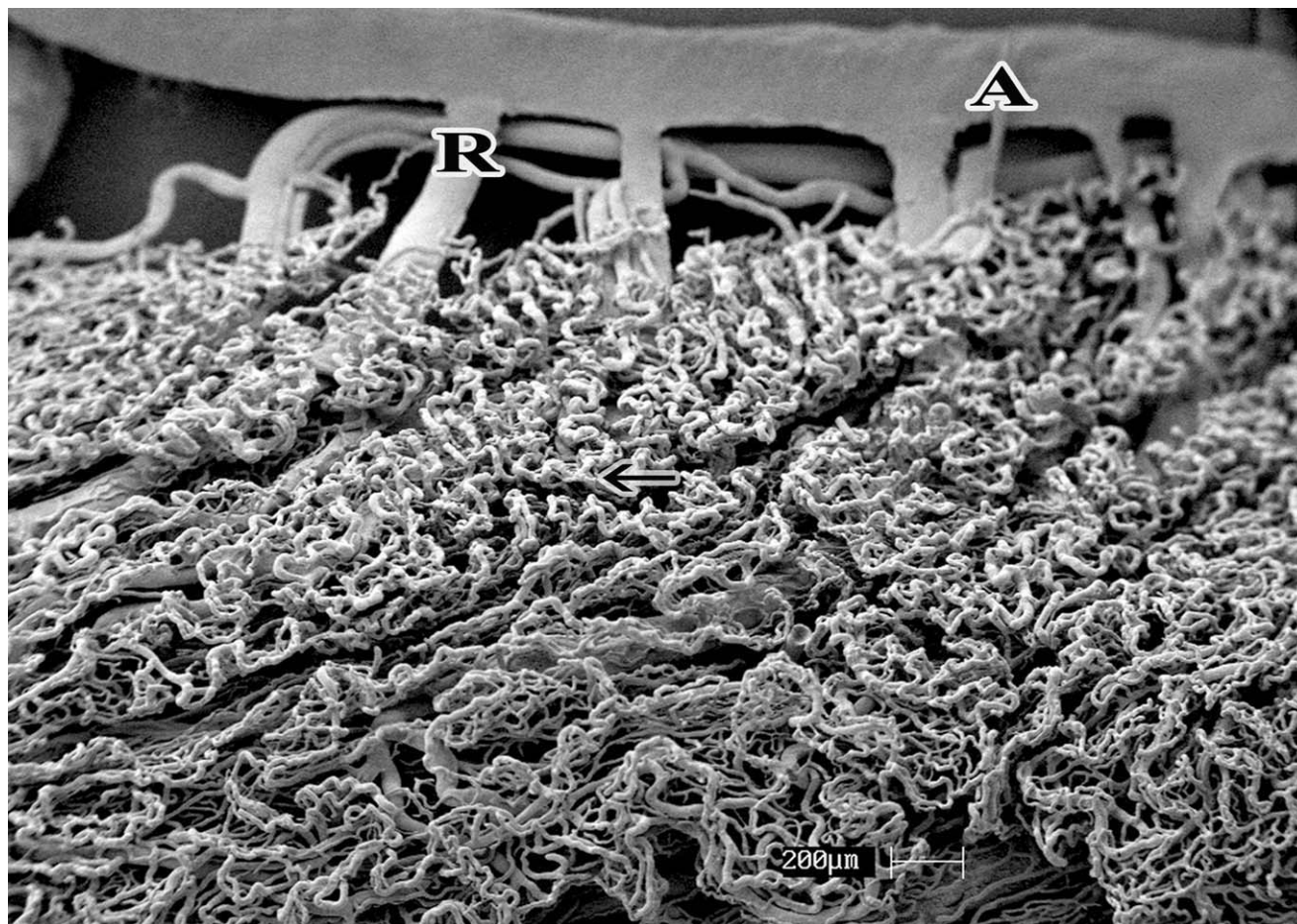


Fig. 1. SEM casts of lateral ventricle CPs. A: rostral choroid artery. R: branch of the rostral choroid artery. The arrow indicates the capillaries of the villous area.

sulfonyl fluoride, 0.1 U/mL aprotinin, 10 mg/mL leupeptin, and 1 mM Na_3VO_4 . Homogenates were centrifuged at 15,000g for 20 min at 4°C. Supernatants were divided into small aliquots and stored at -80°C until used. The amount of total proteins in each sample was determined by Bio-Rad DC protein assay (Bio-Rad Laboratories, Hercules, CA). Samples containing equal amount of proteins were boiled for 5 min in SDS sample buffer (50 mM Tris-HCl, pH 6.8, 2% SDS, 10% glycerol, 0.1% bromophenol blue, and 5% β -mercaptoethanol), and run on a 10% SDS/polyacrylamide gel. After electrophoresis, the proteins were transferred to nitrocellulose using a Mini trans-blot apparatus (Bio-Rad Laboratories) according to the manufacturer's instructions. Membranes were blocked for 1 h at room temperature with TBS-T buffer (150 mM NaCl, 20 mM Tris HCl, pH 7.4, 0.1% Tween 20) containing 5% milk. The blots were incubated overnight with a rabbit polyclonal antibody raised against a peptide mapping the 724–739 amino acid sequence of human brain NOS I (AB1632, Chemicon International, Temecula CA) diluted 1:1,000 in TBS-T containing 2.5% milk. After incubation, membranes were washed three times with TBS-T and incubated for 1 h with horseradish peroxidase conjugated anti-rabbit IgG (Sigma Chemical)

diluted 1:3,000 in TBS-T containing 2.5% milk. The proteins were visualized by enhanced chemiluminescence (ECL; Amersham, Little Chalfont, UK). To ensure specificity, preabsorption of NOS I antibody with its control peptide (AG591, Chemicon International, Temecula CA) was performed before Western blotting. The same blots were stripped and re probed using antitubulin monoclonal antibody (MAB 1637, Chemicon International, Temecula CA) to confirm equal loading of proteins in all lanes.

RESULTS

Anatomy

The CPs of buffalo brain are clearly visible to the naked eye. Each lateral ventricle contains a CP located near the medial wall of the ventricle. Each plexus is C-shaped, and has its C-opening directed laterally. The III ventricle contains a single CP located on the roof of the ventricle. This plexus is caudo-rostrally elongated, and originates from the fusion along the median sagittal axis of the CPs located in the two lateral ventricles. In addition, each plexus exits from an interventricular hole, also known as the Monroe foramen (*Foramen interventriculare*), and fuses with

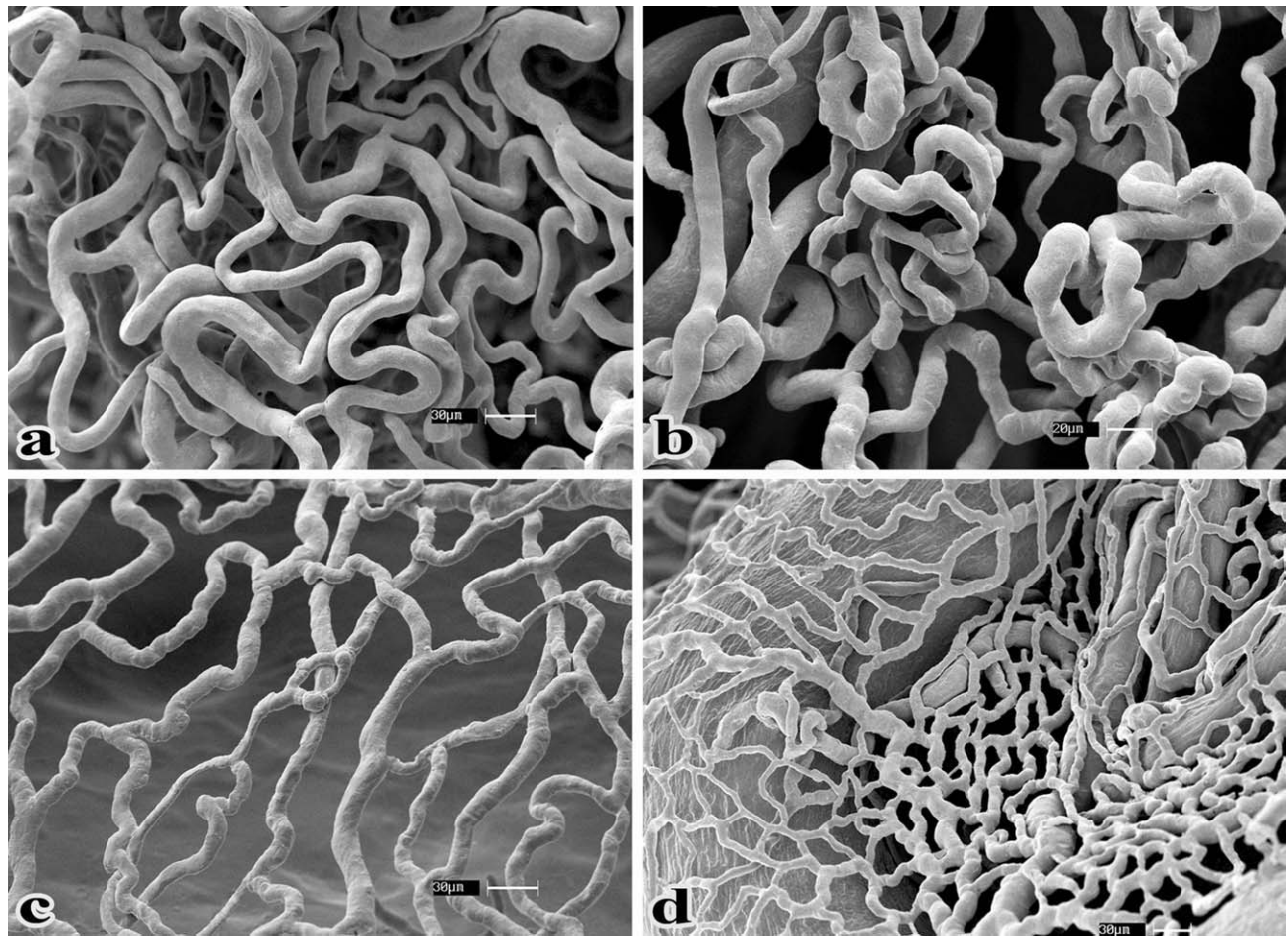


Fig. 2. SEM casts of the lateral ventricle CPs. Different features of the blood capillaries. **a**: arrangement of blood capillaries in flat areas. **b**: blood capillaries of the villi. **c**: network capillaries. **d**: network capillaries that wind around the large upper blood vessels.

the other plexus along the median sagittal axis in the rostral direction. The IV ventricle contains two CPs. Each plexus is an elongated structure located on the roof of the ventricle, and lies along the caudal borders of the ventricle.

SEM-Angioarchitecture

The CP vascular casts of buffalo brain were observed to have either of two shapes: lamina-like and ovoid-like (inflorescence). The lamina-like shape is present in the lateral and III ventricle CPs. The ovoid-like shape is present in the IV ventricle CPs.

Lamina-Like CPs. Arteries. Each lamina-like CP of the lateral ventricle is irrigated by a rostral choroid artery (*A. choroidea rostralis*), which branches off from the median cerebral artery (*A. cerebri media*). These rostral choroid arteries are directed towards the ventral-lateral extremities, and run along the full length of the rostro-ventral border of the CP. During its ventricular run, the choroid artery ramifies into 5 or 6 branches, each one having an inner diameter of about 200 µm, and then further ramifies into capillaries on both sides of the CP. The first branch of the choroid artery is located on

the ventro-lateral extremity of the ventricle, and unfolds in a fan-like manner. The second branch runs along the dorso-caudal border; it is flexuous and ramifies into numerous collateral branches which anastomose with other branches. The third and fourth branches are perpendicular to the dorso-caudal border, and are distributed throughout the central portion of the CP. The remaining branches are distributed throughout the dorso-medial extremity of the CP of each lateral ventricle, and anastomose with the cerebral caudal branches (*Rami choroidei caudales*). The lateral ventricle CPs exit the interventricular hole and form the III ventricle CP, which has a long, laminar shape (about 1 cm) in the caudal direction. The III ventricle CP is irrigated by the caudal branches (*Rami choroidei caudales*) of the caudal cerebral artery (*A. cerebri caudalis*).

Veins. The venous circulation begins at the post capillary small veins (30–40 µm, inner diameter) which either continue directly to the medium and large caliber veins situated along the dorso-caudal border of the lateral ventricles, or to the large cerebral vein (*V. cerebri magna*). The former continue on to the marginal veins, which wind around the two sides of the polygonal stitch capillary network. These marginal

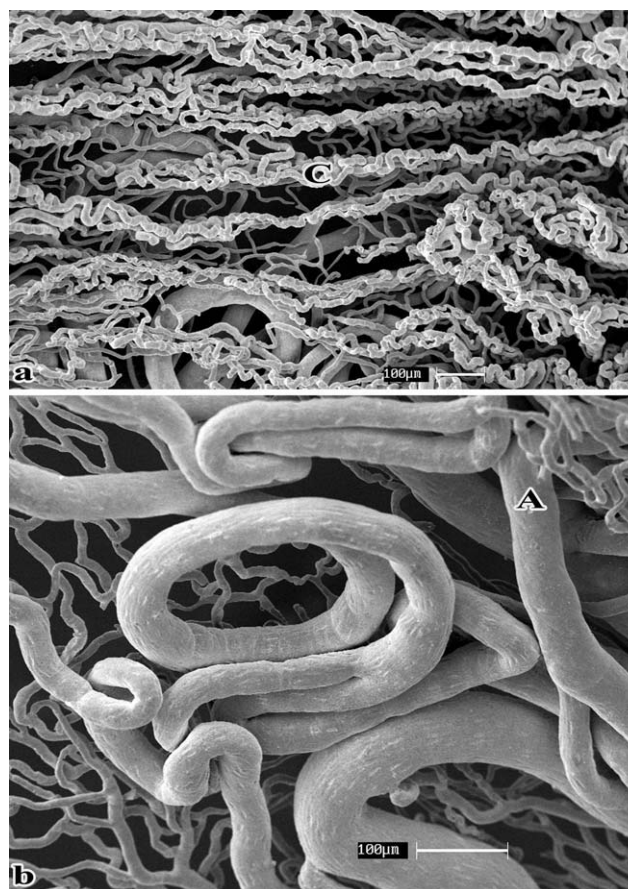


Fig. 3. SEM casts of III ventricle CP. a: blood capillaries like plowed field arrangement. b: blood vessels under capillaries. A: arteriole. C: blood capillaries.

veins then continue on to the dorso-medial extremity of the lateral ventricle CPs, and then on to the inner cerebral veins (*Vv. cerebri internae*) that lead into the large cerebral vein.

Capillaries. The capillaries are the most numerous components of the lateral and III ventricles. In the lateral ventricle, the capillaries are organized in various manners: they are located on both sides of the ventricle and either form villous areas along the lateral extremity and rostro-ventral borders, or follow lines parallel to the rostral-ventral margins, and anastomose with each other forming anastomose with an inner diameter of about 10 μm (Fig. 1). In the remaining parts of the lateral ventricle, the capillaries form a network that winds around the large upper blood vessels (Fig. 2). In the III ventricle, the CP capillaries are dorsal to the arterioles, which form large circular windings, and small veins. The capillaries have the appearance of a continuous furrowed surface, somewhat like a plowed field (Fig. 3).

Ovoid-Like (Inflorescence) Vascularization of the IV Ventricle CPs. There are two ovoid-like CPs, each of which is supplied with blood from a caudal cerebellar artery (*A. cerebellis caudalis*). The vascular branches of each caudal cerebellar artery on the ventral surface of a plexus travel dorsally, and subdivide to form small arteries that connect the ovoid-like CPs to the branches. These small arteries go on to anastomose

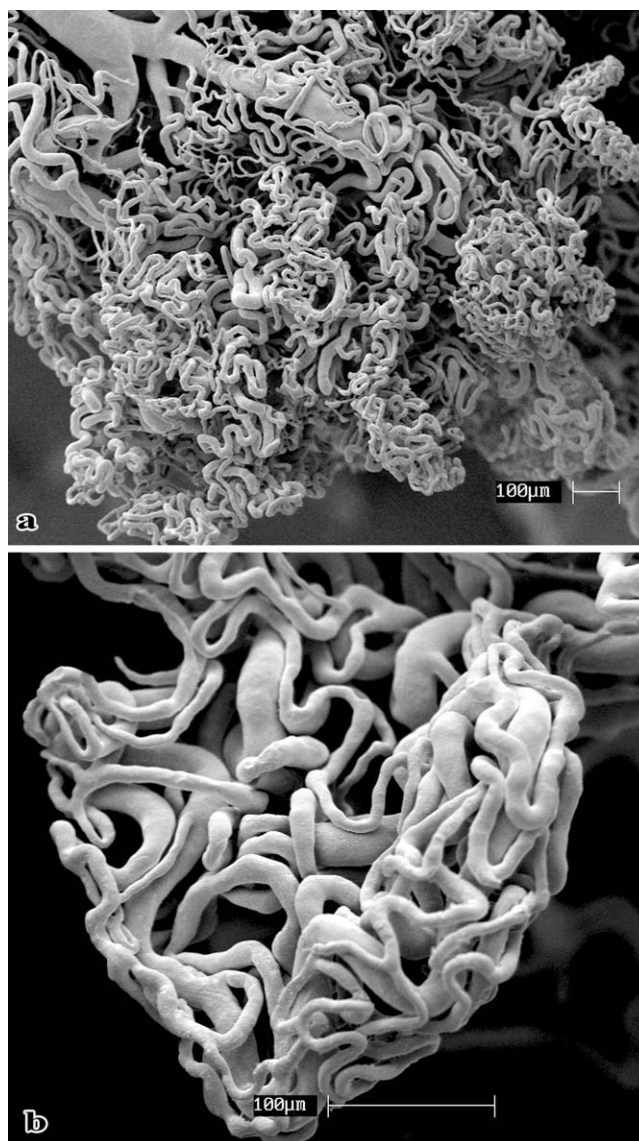


Fig. 4. SEM casts of IV ventricle CPs. a: general arrangement of the blood capillaries. b: blood capillaries of the ovoid-like (inflorescence).

among themselves, thus forming an ovoidal vascularization ($\sim 200 \mu\text{m}$ diameter; Fig. 4). This marks the beginning of the venous drainage system formed by the succession of postcapillary veins, small veins and the veins of the IV ventricle CPs that empty into the ventral cerebellar veins.

Morpho-Structural Features of the CP Capillaries

The morphology of the CP capillaries of the lateral and III ventricle (lamina-like form) showed several typical features: (1) at some points along the capillary run the capillaries took on the shape of either simple-single, or complex-single and double rings of varying dimensions (Fig. 5a); (2) adjacent capillaries were sometimes joined by transversal vascular connections (Fig. 5b); (3) the capillary outer surfaces had single or

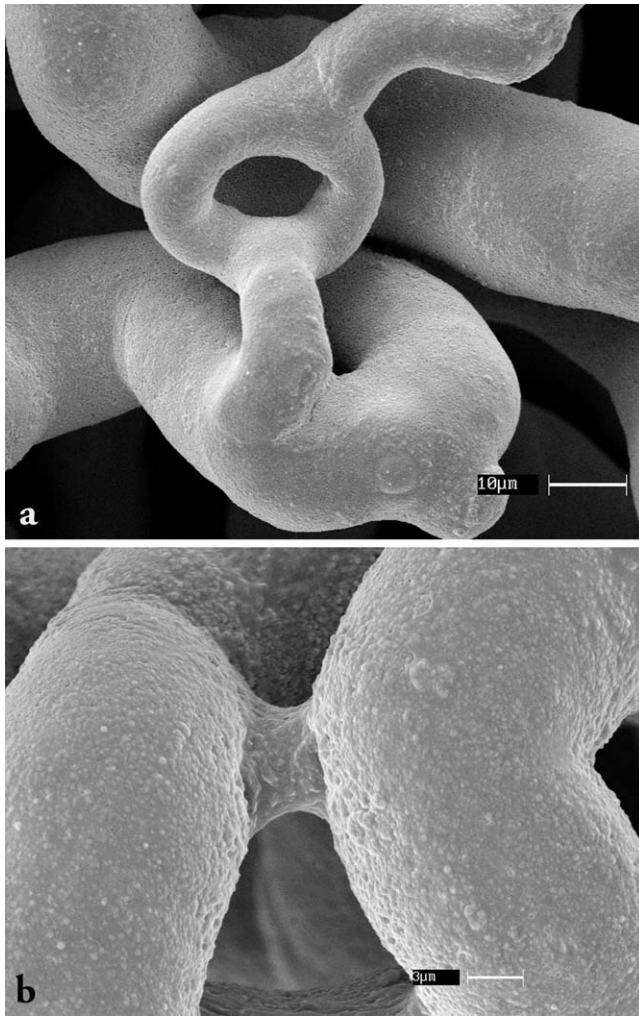


Fig. 5. SEM casts of CPs (lateral and III ventricles). Forms of the vascular rings and vascular connection between adjacent blood capillaries. **a**: simple ring. **b**: vascular connection by short capillaries.

double button shaped extrusions ($\sim 7\text{--}8\ \mu\text{m}$ diameter) delimited by deep furrows, and to which elongated cellular elements were attached (Fig. 6); (4) the capillary inner surfaces showed two types of cellular walls at high SEM magnifications: noncontinuous (porous), and continuous. The diameter of each pore was $\sim 100\ \mu\text{m}$, and each drop of micropinocytosis, which composed the continuous walls was ~ 200 to $300\ \mu\text{m}$ in diameter (Fig. 7); (5) the inner surface of the capillaries was seen under TEM to be composed of a thin layer of endothelial cells which lay on the basal membrane. These endothelial cells had numerous fenestrations which were bridged by a thin membrane, or diaphragm, and which contained pinocytotic vesicles. The external surface of the capillaries had button shaped extrusions that served as anchor points for the elongated cells of the choroid epithelium (Fig. 8).

Histochemistry and Immunohistochemistry of the Blood Capillaries in the CPs

The histochemical analysis of the NADPHd tissue sections from the CPs blood vessels showed an intense

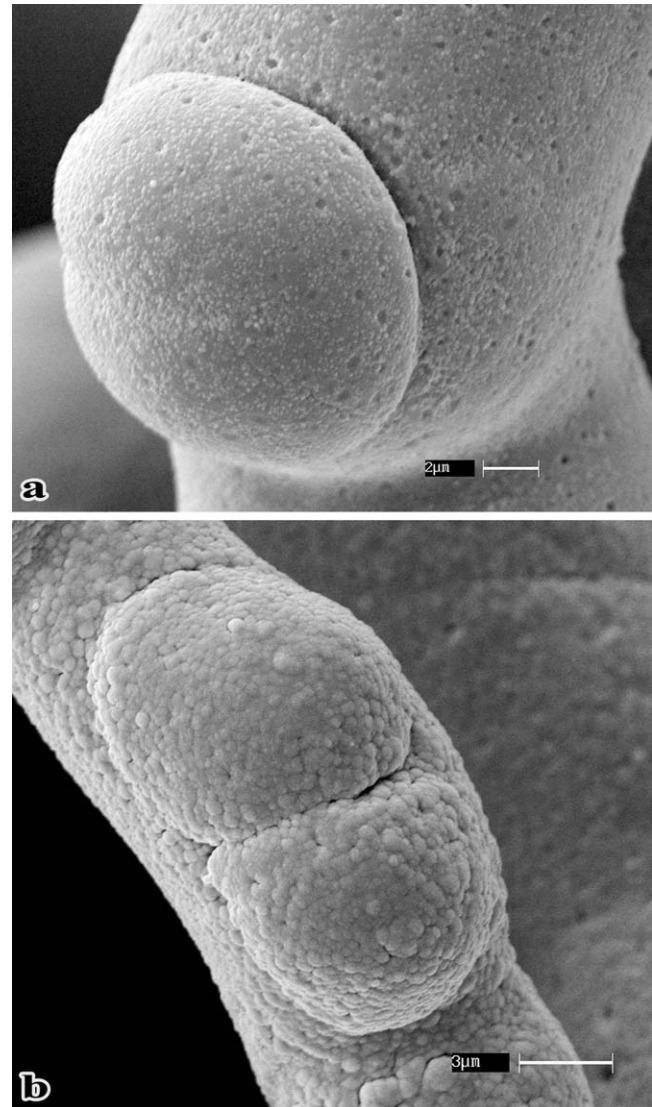


Fig. 6. SEM casts of CPs (lateral and III ventricle). Hallmark of the sticking points of the elongated cell to the blood capillary. **a**: simple button-like formation. **b**: double button-like formation.

staining. The color was more intense in the samples exposed to enzymatic reaction for long time periods at room temperature. The microscopy photographs of these stained tissue sections showed blood capillaries containing an intense staining of the intima, and a rich nitroergic nervous component along the capillaries. This component consisted of elongated bipolar neurons that covered the capillary with their prolongations. In addition, tissue sections of the small veins showed a thin colored muscular layer that circled around the vein (Fig. 9). The immunogold-labeling in SEM of NOS I of the blood capillaries of the CPs showed NOS I-positive particles present either in groups or distributed singularly along the wall of the blood vessels (Fig. 10). No immunoreactivity was observed in the samples treated with PBS instead of the primary antibody (negative control). The expression of NOS I in the CPs was confirmed by immunoblotting using a specific rabbit poly-

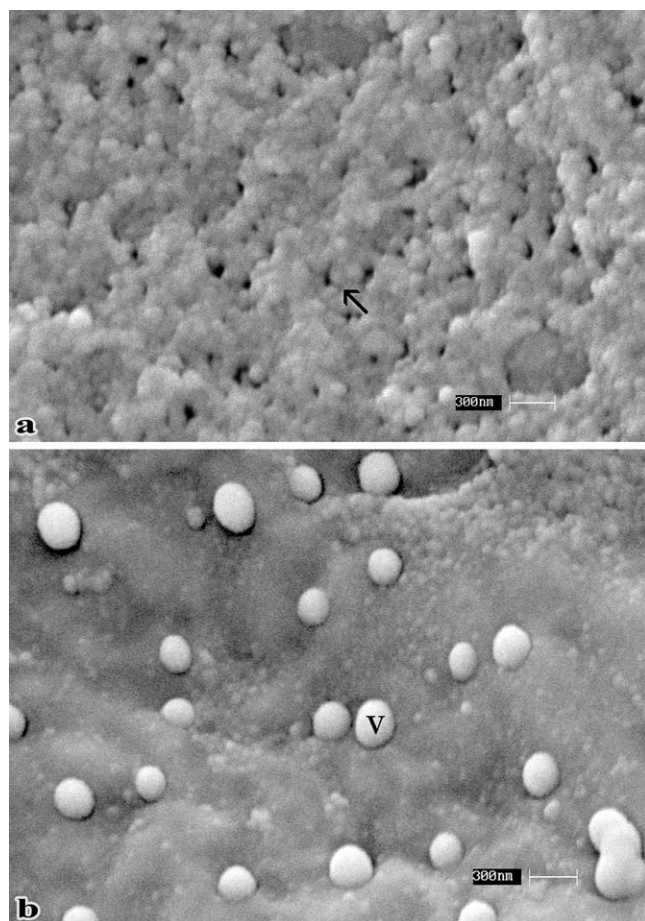


Fig. 7. The SEM intact tissue technique. Luminal surface of the endothelium. **a**: fenestrations of endothelium. **b**: pinocytotic vesicles. V: contents pinocytotic vesicles. The arrow indicates the fenestrations of the luminal surface of the epithelium.

clonal antibody raised against a peptide mapping of the 724–739 amino acid sequence of human brain NOS I. The protein detected had a molecular mass of ~155 kDa, which is consistent with the molecular mass of NOS I (125–160 kDa) found in the brain of various mammalian species. The specificity of the response was confirmed by the precipitation of the NOS I antibody with its blocking peptide [see (Scala et al., 2007)].

DISCUSSION

In general, SEM and TEM analyses of the CPs from buffalo brain showed morphological and structural features similar to those reported in other mammalian species (Adami et al., 2005; De Spiegelaere et al., 2008; Gomez and Potts, 1981; Miodonski et al., 1979; Peters and Swan, 1979; Rajtovà, 2002; Scala et al., 1994; Tamega et al., 2000; Webster, 1976). The blood microvasculature is the major component of the CPs responsible for the formation of the CSF. In mammals, 90% of the CSF is secreted by the encephalic CPs (Spector and Johanson, 1989). This fluid plays an important role in maintaining brain homeostasis. In turn, the chemical composition and quantity of this fluid depends on several morpho-functional characteristics

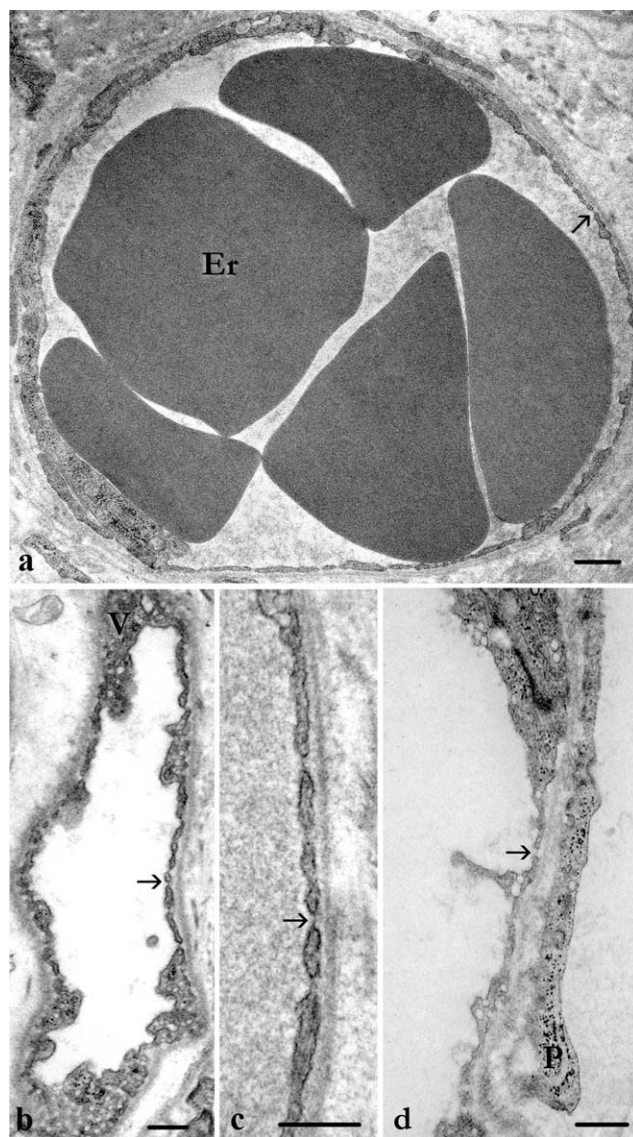


Fig. 8. TEM blood capillary of CP. **a**: cross section of true blood capillary. **b**: blood capillary with intense functional activity. **c**: fenestrations with closing membrane. **d**: extended cellular element project its peduncle towards the endothelium. Er: erythrocyte. P: peduncle of elongated cell. V: pinocytotic vesicles. The arrows indicate the fenestrations of the luminal surface of epithelium. Scale bars = 1 μ m.

of the vascularization of the CPs. These characteristics are as follows:

1. The two shapes of the vascular organization (lamina-like and ovoid-like) of the CP capillaries corresponded to the two shapes of the ventricular cavities. In addition, the lamina-like vascular organization was composed of various types of vascular suborganizations (anastomotic networks, villous capillary masses on the flat surfaces, and capillary networks that wrap around the blood vessels), and the ovoid-like vascular suborganization (anastomotic) was composed of ovoid formations of varied dimensions. On the basis of these two types of vascular organizations it may be hypothesized that the

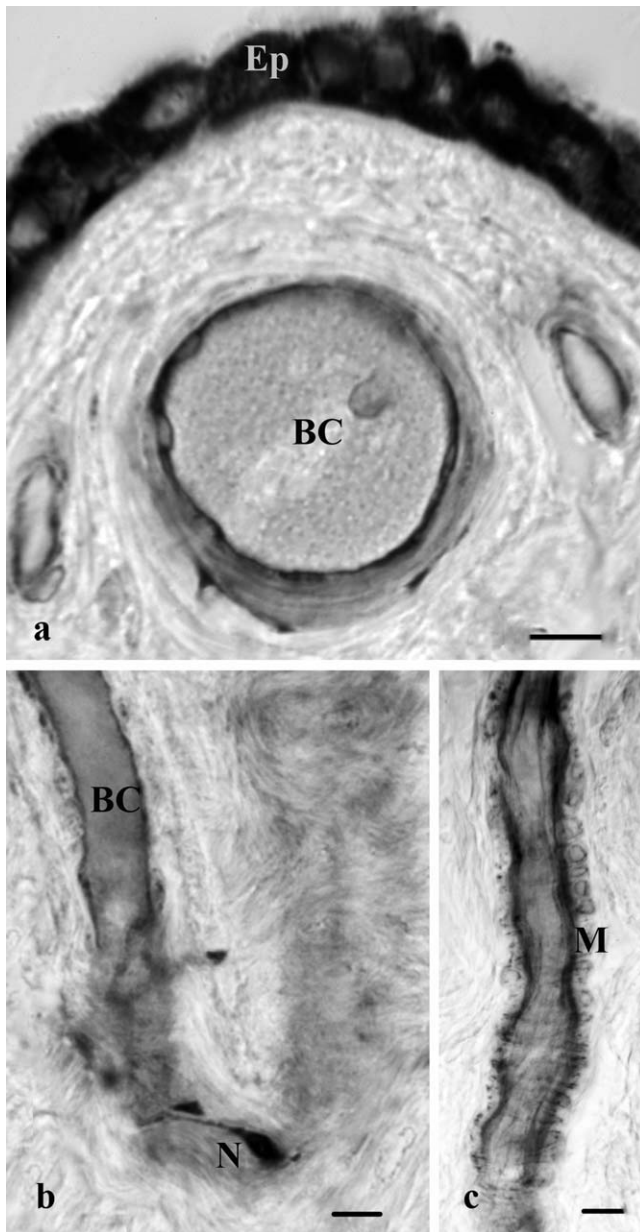


Fig. 9. LM-NADPHd of the CP. **a**: epithelium and blood capillary. **b**: nitroergic nervous component of blood capillary. **c**: muscular layer of small vein. BC: blood capillary. Ep: choroid epithelium. M: muscular fiber. N: nitroergic innervation. Scale bars = 5 μ m.

capillaries of the CPs are highly dynamic formations that change their organization in response to the changing exigencies of the CNS internal microenvironment.

2. Elongated cells of the CPs, which have both a peduncular portion and a globular portion, enter into the ventricular cavity. These cells connect the ventricular cavities to the blood capillaries. On the basis of this connection it can be hypothesized that these elongated cells serve to monitor changes in the chemical composition of the CSF, and to control the flow of micronutrients and microelements across the vascular endothelium and the choroid epithelium.

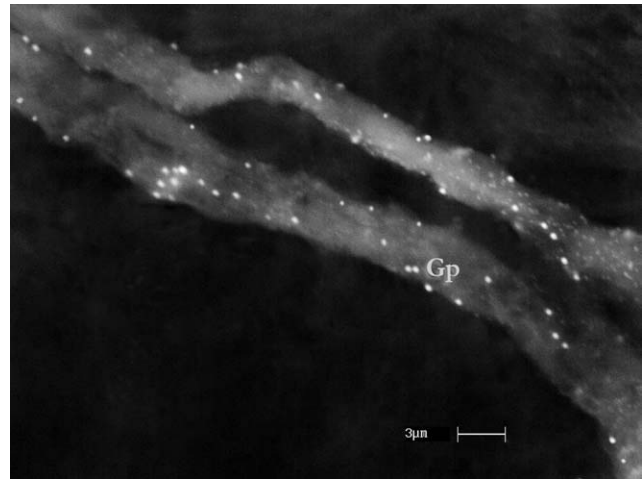


Fig. 10. The SEM-NOS I immunoreactive blood capillary of the CP. Gp: gold particles.

3. The capillaries of the CPs have diverse forms; they can anastomose among themselves, or form single and multiple vascular rings, or form spirals that frequently subdivide into branches. It can be hypothesized that these diverse forms correspond to the diverse chemical conditions of the CSF. This hypothesis presents a dynamic view of the blood capillaries.
4. The presence of many annular windings in the CPs that anastomose among themselves leads to the hypothesis that these windings are involved in the secretion and absorption of the CSF so as to maintain the pressure of the CP blood vessels stable, independently of the blood pressure conditions outside of the brain. This hypothesis is consistent with the results of Kadel et al. (1990), which reported that endothelin reduces the flow of blood in CPs and dura mater without any effects on cerebral blood flow.
5. The SEM and TEM examinations of the CP vessels showed the presence of two types of internal wall surfaces in the capillaries: fenestrated and nonfenestrated. This observation leads to the hypothesis that these surfaces are involved in the major functions of the CPs, namely, in the secretion and absorption of the CSF. A previous study (Spector and Johanson, 1989) states that the CPs function as a kidney for the brain insofar as they maintain the chemical stability of the CFS. If this hypothesis is true, it may be further deduced that the CPs also maintain the stability of the micro-environment of CNS.
6. The present study of the CPs has used indirect evidence to show the presence of NO in the CPs, specifically, the presence of NADPHd and NOS I was taken as indirect evidence for the presence of NO. A previous study by Marletta (1993) confirms the validity of the indirect evidence; he demonstrated that NOS I produces NO and citrulline from arginine, molecular oxygen and NADPH. In addition, other studies have used this indirect method of evidencing NO, for example, Faraci and Heistad (1992) in their investigation of the specific role of NO in the CPs.
7. The present study, by using the immuno-gold technique for SEM, has shown a strong NOS I immuno-

reactivity in the walls of CP blood vessels, and hence, the presence of NO. Other researchers, using other techniques have associated the presence of NO in the cerebral arteries of various animals with a vaso-dilatory function: in humans, Toda (1993); in monkey, Toda and Okamura (1990c) and Toda et al. (1996); in dog, Toda and Okamura (1990a,b; 1991; 1993); in pig, Lee and Sarwinski (1991) and Tanaka et al. (1999); in cow, Gonzalez and Estrada (1991) and Ayajiki et al. (1993); in cat, Ayajiki et al. (1994), in sheep, Matthew and Wadsworth (1997); in guinea pig Jiang et al. (1997), and in rat, Ignacio et al. (1997).

In addition, the NO is involved in autoregulation of vascular tone by cholinergic nerve stimulation of blood vessel smooth muscle (Toda and Okamura, 2003). The results and hypotheses of our study will hopefully contribute to further research aiming to elucidate the mechanisms by which the CPs regulate the production of CSF, which in turn stabilizes the microenvironment inside the CNS.

REFERENCES

- Adami M, Faria MM, Almeida AE, Pinto MG, Prada IL. 2005. Scanning electron microscopy of the choroid plexus of the lateral ventricle of the horse. *Anat Histol Embryol* 34:379–382.
- Ayajiki K, Okamura T, Toda N. 1993. Nitric oxide mediates and acetylcholine modulates neurally induced relaxation of bovine cerebral arteries. *Neuroscience* 54:819–825.
- Ayajiki K, Okamura T, Toda N. 1994. Neurogenic relaxations caused by nicotine in isolated cat middle cerebral arteries. *J Pharmacol Exp Ther* 270:795–801.
- Cumming R, Cheung WY, Wallace RW, Steiner AL. 1981. Immunofluorescent localization of cyclic GMP, calmodulin plexus of rat and mouse. *Neurosci Lett* 28:119–124.
- Dawson VL, Dawson TM. 1996. Nitric oxide synthase: Role as a transmitter/mediator in the brain and endocrine system. *Annu Rev Med* 47:219–227.
- De Spiegelaere W, Casteleyn C, Van Den Braeck WSimoens P. 2008. Electron microscopic study of the porcine choroid plexus epihelium. *Histol Embryol* 37:458–463.
- Faraci FM, Heistad DD. 1992. Does basal production of nitric oxide contribute to brain-fluid balance? *Am J Physiol* 262:340–344.
- Feldman PL, Griffith OW, Stuehr DJ. 1993. The surprising life of nitric oxide. *Chem Eng News* 20:26–38.
- Gomez DG, Potts DG. 1981. The lateral, third and fourth ventricle choroid plexus of the dog: A structural and ultrastructural study. *Ann Neurol* 10:333–340.
- Gonzalez C, Estrada C. 1991. Nitric oxide mediates the neurogenic vasodilatation of bovine cerebral arteries. *J Cereb Blood Flow Metab* 11:366–370.
- Hirooka K, Kourenny DE, Barnes S. 2000. Calcium channel activation facilitated by nitric oxide in retinal ganglion cells. *J Neurophysiol* 83:198–206.
- Hope BT, Michael GJ, Knigge KM, Vincent SR. 1991. Neuronal NADPH-d is a nitric oxide synthase. *Proc Natl Acad Sci USA* 88:2811–2814.
- Ignacio CS, Curling PE, Childres WF, Bryan RM. 1997. Nitric oxide-synthesizing perivascular nerves in the rat middle cerebral artery. *Am J Physiol* 273:R661–R668.
- Jiang F, Li CG, D Rand MJ. 1997. Mechanism of electrical field stimulation-induced vasodilatation in the guinea pig basilar artery: The role of endothelium. *J Auton Pharmacol* 17:71–76.
- Kadel KA, Heistad DD, Faraci FM. 1990. Effects of endothelin on blood vessels of the brain and choroid plexus. *Brain Res* 518:78–82.
- Lee TJ-F, Sarwinski SJ. 1991. Nitric oxidergic neurogenic vasodilatation in the porcine basilar artery. *Blood Vessels* 28:407–412.
- Marletta MA. 1993. Nitric oxide synthase structure and mechanism. *J Biol Chem* 268:12331–12334.
- Matthew JD, Wadsworth RM, McPhaden AR. 1997. Inhibition of vasodilator neurotransmission in the sheep middle cerebral artery by VIP antiserum. *J Auton Pharmacol* 17:971–973.
- Miodonski A, Poborowska J, Friedhuber de Grubenthal A. 1979. SEM study of the choroid plexus of the lateral ventricle in the cat. *Anat Embryol (Berlin)* 155:323–331.
- Moncada S, Higgs EA. 2006. The discovery of nitric oxide and its role in vascular biology. *Br J Pharmacol* 147:193–201.
- Ohtani O, Gannon B, Ohtsuka A, Murakami T. 1982. The microvasculature of bone and especially of bone marrow as studied by scanning electron microscopy of vascular casts a review. *Scan Electron Microsc* 1:427–434.
- Owen GRH, Meredith DO, Gwynn I, Richards RG. 2002. Simultaneously identifying S-phase labelled cells and immunogold-labelling of vinculin in focal adhesions. *J Microsc* 207:27–36.
- Pavone LM, Tafuri S, Mastellone V, Della Morte R, Lombardi P, Avallone L, Maharajan V, Staiano N, Scala G. 2007. Expression of the serotonin transporter (SERT) in the choroid plexuses from buffalo brain. *Anat Rec* 290:1492–1499.
- Peters A, Swan RC. 1979. The choroid plexus of the mature and aging rat: The choroidal epithelium. *Anat Rec* 194:325–354.
- Rajtovà V. 2002. Scanning electron microscopy of plexus choroideus in adult sheep. *Acta Vet Brno* 71:279–282.
- Richards RG, Stiffanic M, Owen GRH, Riehle M, Gwynn JAP, Curtis ASG. 2001. Immunogold labelling of fibroblast focal adhesion sites visualized in fixed material using scanning electron microscopy. *Cell Biol Int* 2:1237–1249.
- Scala G, Mirabella N, Paino G, Pelagalli GV. 1994. Sur la microvascularization des plexus choroïdes des ventricules latéraux chez la chèvre (*Capra hircus*). *Anat Histol Embryol* 23:93–101.
- Scala G, Corona M, Pavone LM, Pelagalli A, de Girolamo P, Staiano N. 2007. Structural and functional features of choroid epithelium from buffalo brain. *Anat Rec* 290:1399–1412.
- Spector R, Johanson CE. 1989. The mammalian choroid plexus. *Sci Am* 261:68–74.
- Tafuri S, Pavone LM, Mastellone V, Spina A, Avallone L, Vittoria A, Staiano N, Scala G. 2009. Expression of orexin A and its receptor 1 in the choroid plexuses from buffalo brain. *Neuropeptides* 43:73–80.
- Tamega OJ, Tirapelli LF, Petroni S. 2000. Scanning electron microscopy study of the choroid plexus in the monkey. *Arq Neuropsiquiatr* 58:820–825.
- Tanaka T, Okamura T, Handa J, Toda N. 1999. Neurogenic vasodilatation mediated by nitric oxide in porcine cerebral arteries. *J Cardiovasc Pharmacol* 33:56–64.
- Toda N. 1993. Mediation by nitric oxide of neurally-induced human cerebral artery relaxation. *Experientia (Basel)* 49:51–53.
- Toda N, Okamura T. 1990a. Modification by L-N^G-monomethyl arginine (L-NMMA) of the response to nerve stimulation in isolated dog mesenteric and cerebral arteries. *Jpn J Pharmacol* 52:170–173.
- Toda N, Okamura T. 1990b. Possible role of nitric oxide in transmitting information from vasodilator nerve to cerebroarterial muscle. *Biochem Biophys Res Commun* 170:308–313.
- Toda N, Okamura T. 1990c. Mechanism underlying the response to vasodilator nerve stimulation in isolated dog and monkey cerebral arteries. *Am J Physiol* 259:H1511–H1517.
- Toda N, Okamura T. 1991. Role of nitric oxide in neurally induced cerebroarterial relaxation. *J Pharmacol Exp Ther* 258:1027–1032.
- Toda N, Okamura T. 1993. Responses to perivascular nerve stimulation of distal temporal arteries from dogs and monkeys. *J Cardiovasc Pharmacol* 22:744–749.
- Toda N, Okamura T. 1996. Monkey central retinal artery is innervated by nitroxidergic vasodilator nerves. *Invest Ophthalmol Vis Sci* 37:2177–2184.
- Toda N, Okamura T. 2003. The pharmacology of nitric oxide in the peripheral nervous system of blood vessels. *Pharmacol Rev* 55:271–324.
- Webster HF. 1976. Choroid plexus. In: Peters A, Palay SL, Webster HF, editors. *The fine structure of the nervous system: The neurons and supporting cells*. Philadelphia: Saunders. pp. 280–294.